

Hemoglobin–oxygen–carbon monoxide equilibria with the MWC model

N.M. Senozan*, J.A. DeVore, E.K. Lesniewski

Department of Chemistry and Biochemistry, California State University, Long Beach, CA 90840, USA

Received 10 June 1998; received in revised form 1 September 1998; accepted 2 September 1998

Abstract

Fractional saturation equations for the Monod, Wyman and Changeux model are derived for the case of two distinct ligands bonding to a host molecule with four ligand sites and two conformational states. A variety of useful graphical studies can be derived from these equations when applied to normal human hemoglobin with O₂ and CO as ligands. For example, the oxygen transport capability of hemoglobin can be assessed at different environmental CO levels and the concentrations of various liganded species can be displayed as a function of fractional saturation with oxygen. In addition, the CO pressure in the tissue, $p_{\text{CO}}^{\text{tissue}}$, can be calculated as a function of the tissue oxygen pressure, $p_{\text{O}_2}^{\text{tissue}}$, at different environmental levels of CO. In an environment of a given CO concentration, $p_{\text{CO}}^{\text{tissue}}$ decreases with $p_{\text{O}_2}^{\text{tissue}}$ until a minimum is reached. Further decrease in $p_{\text{O}_2}^{\text{tissue}}$ results in a fairly steep rise in $p_{\text{CO}}^{\text{tissue}}$. © 1998 Elsevier Science B.V. All rights reserved.

Keywords: Hemoglobin; Carboxyhemoglobin; MWC; Monod, Wyman and Changeux; Oxygenation curves

1. Introduction

Quantitative studies of the equilibrium between carbon monoxide and hemoglobin date back to the work of Douglas et al. [1]. Their observations led to the general statements that have become known as Haldane's laws. According to Haldane's first law, for a hemoglobin solution equilibrated

with a mixture of oxygen and carbon monoxide,

$$\frac{N_{\text{CO}}}{N_{\text{O}_2}} = M \left(\frac{p_{\text{CO}}}{p_{\text{O}_2}} \right)$$

where N_{CO} and N_{O_2} are the number of bound moles of CO and O₂; p_{CO} and p_{O_2} are the partial pressures of these gases and M is a constant whose value is approximately 220 for human hemoglobin. This relation appeared to be true regardless of the extent of saturation with ligand, i.e. independent of the amount of unliganded

* Corresponding author.

hemoglobin in the solution. Haldane's second law stipulates that when hemoglobin is exposed to a mixture of CO and O₂, the total saturation is a function of $p_{O_2} + M \cdot p_{CO}$ alone, in other words, for a given value of $p_{O_2} + M \cdot p_{CO}$, the fraction of unliganded hemoglobin remains constant regardless of the relative proportions of oxygen and carbon monoxide. Haldane's treatment of the Hb–O₂–CO equilibrium was extended by Roughton and Darling [2] who developed a method of determining oxygenation curves in the presence of carbon monoxide from a knowledge of N_{CO} alone. The method of Roughton and Darling has been widely used to assess hemoglobin's effectiveness as an oxygen carrier and the dissociation curves derived from it continue to be a primary tool of physiologists in understanding respiratory consequences of carboxyhemoglobin in blood [3–5].

The objective of this paper is to show that for the Monod, Wyman and Changeux (MWC) model, saturation curves for oxygen in the presence of carbon monoxide can be derived using only combinatorial arguments and to present these curves in ways suitable for discussing the physiological consequences of the Hb–O₂–CO equilibrium. The original MWC model, in which a polymeric protein is assumed to exist in two or more conformational states, has been very useful in explaining the behavior of regulatory enzymes and the binding of oxygen to respiratory molecules [6–17]. This model offers a number of advantages over the Haldane approach. It yields analytical expressions for the saturation curves and eliminates a cumbersome feature of the Haldane–Roughton method — the necessity of computing oxygen curves point by point. Furthermore, equations derived from the MWC model can be adjusted for various conditions by proper selection of the parameters of the model. The model incorporates Haldane's laws as a special case when the ratio of the affinities for the two ligands is the same in each conformational state, but is not constrained to assume that the coefficient M remains independent of the extent of saturation. There is in fact considerable evidence that M varies and that Haldane's laws are valid only for compositions in which hemoglobin is nearly saturated with one

ligand [15–18]. Finally, the MWC model provides convenient analytical expressions from which concentrations of various ligated hemoglobin species can be calculated. It is interesting to note that doubly and especially triply ligated hemoglobin molecules exist at very low concentrations over the entire saturation ranges of oxygen or carbon monoxide. The low levels of these intermediate species are an inherent feature of the strong allosteric nature of the MWC model and it is not necessary to invoke any special molecular properties to explain their scarcity.

Analytical expressions derived in this study not only permit an evaluation of hemoglobin as a transporter of oxygen in the presence of carbon monoxide, but also reveal an interesting feature of carbon monoxide physiology that might not have been noted before. At a given carboxyhemoglobin concentration in blood, the tissue CO pressure, p_{CO}^{tissue} , steadily drops as the tissue oxygen pressure diminishes until a certain $p_{O_2}^{tissue}$ is reached. Below this $p_{O_2}^{tissue}$, as the tissue is further deprived of oxygen, p_{CO}^{tissue} starts rising. Depending on the ambient carbon monoxide pressure, this rise can be quite steep and the p_{CO}^{tissue} may increase by as much as a factor of two relative to its minimum value.

2. The model

With $R_{i,j}$ and $T_{i,j}$ representing the conformational states of hemoglobin with, respectively, i and j molecules of two ligands A_1 and A_2 , i.e. $T_{i,j} = \text{Hb}^T(A_1)_i(A_2)_j$, equilibria for the addition of a ligand to the macromolecule are represented in terms of species concentrations and ligand partial pressures as

$$\frac{[R_{i+1,j}]}{[R_{i,j}]} = \left(\frac{4-i-j}{i+1} \right) K_1^R P_1$$

$$\frac{[T_{i+1,j}]}{[T_{i,j}]} = \left(\frac{4-i-j}{i+1} \right) K_1^T P_1$$

$$0 \leq i \leq 3, 0 \leq j \leq 4-i \quad (1)$$

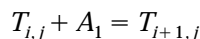
and

$$\frac{[R_{i,j+1}]}{[R_{i,j}]} = \left(\frac{4-j-i}{j+1} \right) K_2^R P_2$$

$$\frac{[T_{i,j+1}]}{[T_{i,j}]} = \left(\frac{4-j-i}{j+1} \right) K_2^T P_2$$

$$0 \leq j \leq 3, 0 \leq i \leq 4-j.$$

where P_1 and P_2 are the equilibrium pressures of the two ligands. For a particular conformation, the affinity of the protein for a ligand is given by an intrinsic equilibrium constant, e.g. K_1^T , which is unaffected by the number of molecules A_1 and A_2 already bonded. The multiplicative factors associated with the intrinsic equilibrium constants in Eq. (1) take into account that on a purely statistical basis, the various equilibria are not all the same. For instance, a hemoglobin molecule with two ligands of type A_1 has two remaining sites onto which a third molecule can bond yielding a product with three sites from which an A_1 molecule may dissociate. The statistical factor for this case is $(4-i-j)/(i+1) = 2/3$. These factors may be considered also as the ratio of two terms, each being the number of ways the bonded molecules may be arranged on a macromolecule with four ligand sites. For example, the multiplicative factor assigned to the reaction



is

$$\frac{(4)!}{(4-i-j-1)!(i+1)!(j)!} / \frac{(4)!}{(4-i-j)!(i)!(j)!}$$

The original MWC model makes no distinction between the α and the β protein chain subunits of hemoglobin and assumes that the two conformational states of the molecule are equilibrated so that one additional equilibrium equation

$$L = [T_{0,0}]/[R_{0,0}] \quad (2)$$

is required. All possible equilibria between different species and conformations can then be written in terms of Eqs. (1) and (2) and the

concentrations of all species can be expressed in terms of the five equilibrium constants, ligand pressures and the concentration of one arbitrarily chosen species, $R_{0,0}$. For example,

$$[R_{2,2}] = \left(\frac{1}{2} \right) (K_2^R P_2) [R_{2,1}] = (K_2^R P_2)^2 [R_{2,0}]$$

$$= \left(\frac{3}{2} \right) (K_1^R P_1) (K_2^R P_2)^2 [R_{1,0}]$$

$$= 6 (K_1^R P_1)^2 (K_2^R P_2)^2 [R_{0,0}]$$

Similarly, with the definitions $c_1 \equiv K_1^T/K_1^R$ and $c_2 \equiv K_2^T/K_2^R$,

$$[T_{2,2}] = 6 L (c_1 K_1^R P_1)^2 (c_2 K_2^R P_2)^2 [R_{0,0}]$$

With $\alpha_1 = K_1^R P_1$ and $\alpha_2 = K_2^R P_2$, an examination of several examples suggests that species concentrations may be written in general as

$$[R_{i,j}] = \frac{(4)!}{(4-i-j)!(i)!(j)!} (\alpha_1)^i (\alpha_2)^j [R_{0,0}] \quad (3a)$$

and

$$[T_{i,j}] = \frac{(4)!}{(4-i-j)!(i)!(j)!} L$$

$$\times (c_1 \alpha_1)^i (c_2 \alpha_2)^j [R_{0,0}] \quad (3b)$$

The fractional saturation, Y_1 , is defined as the number of moles of ligand A_1 bound to the protein per unit volume, N_{A_1} , divided by the number of moles of sites available to A_1 per unit volume, N_{Σ_1} , i.e. the total number of binding sites, N_{Σ} , minus the number occupied by the ligand, A_2 ;

$$Y_1 = \frac{\sum_{j=0}^3 \sum_{i=1}^{4-j} i [R_{i,j}] + [T_{i,j}]}{\sum_{j=0}^3 \sum_{i=0}^{4-j} (4-j) \{ [R_{i,j}] + [T_{i,j}] \}} \quad (4)$$

The total number of binding sites (moles per unit volume) for the two-state hemoglobin model is

given by

$$N_{\Sigma} = 4 \sum_{j=0}^4 \sum_{i=0}^{4-j} \{ [R_{i,j}] + [T_{i,j}] \}$$

With Eqs. (3a) and (3b), the numerator of Eq. (4) can be written in dimensionless form as

$$\begin{aligned} N'_{A_1} &= \frac{N_{A_1}}{4[R_{0,0}]} \\ &= \sum_{j=0}^3 \sum_{i=1}^{4-j} \left[\frac{(3)!}{(4-i-j)!(i-1)!(j)!} \right] \\ &\quad \times [\alpha_1^i \alpha_2^j + L(c_1 \alpha_1)^i (c_2 \alpha_2)^j]. \end{aligned} \quad (5)$$

Let $l = i - 1$ and $k = j + l$. Then

$$\begin{aligned} N'_{A_1} &= \sum_{k=0}^3 \sum_{l=0}^k \left[\frac{(3)!}{(3-k)!(k-l)!(l)!} \right] \\ &\quad \times [\alpha_1^{l+1} \alpha_2^{k-l} + L(c_1 \alpha_1)^{l+1} (c_2 \alpha_2)^{k-l}]. \end{aligned} \quad (6)$$

Multiplying and dividing by $k!$ and using the notation for binomial coefficients, Eq. (6) becomes

$$\begin{aligned} N'_{A_1} &= \sum_{k=0}^3 \binom{3}{k} \left[\alpha_1 \sum_{l=0}^k \binom{k}{l} \alpha_1^l \alpha_2^{k-l} \right. \\ &\quad \left. + L c_1 \alpha_1 \sum_{l=0}^k \binom{k}{l} (c_1 \alpha_1)^l (c_2 \alpha_2)^{k-l} \right]. \end{aligned}$$

Introducing unity as $(1)^{3-k}$, we have

$$\begin{aligned} N'_{A_1} &= \alpha_1 \sum_{k=0}^3 \binom{3}{k} (1)^{3-k} (\alpha_1 + \alpha_2)^k \\ &\quad + L c_1 \alpha_1 \sum_{k=0}^3 \binom{3}{k} (1)^{3-k} (c_1 \alpha_1 + c_2 \alpha_2)^k, \end{aligned} \quad (7)$$

which immediately yields

$$\begin{aligned} N'_{A_1} &= \alpha_1 (1 + \alpha_1 + \alpha_2)^3 \\ &\quad + L c_1 \alpha_1 (1 + c_1 \alpha_1 + c_2 \alpha_2)^3. \end{aligned} \quad (8)$$

With Eqs. (3a) and (3b) and after multiplying and dividing by $(3-j)!$, the denominator of Eq. (4) becomes

$$\begin{aligned} N'_{\Sigma_1} &= \frac{N_{\Sigma_1}}{4[R_{0,0}]} \\ &= \sum_{j=0}^3 \left[\frac{(3)!}{(3-j)!(j)!} \right] \sum_{i=0}^{4-j} \left[\frac{(4-j)!}{(4-i-j)!(i)!} \right] \\ &\quad \times [\alpha_1^i \alpha_2^j + L(c_1 \alpha_1)^i (c_2 \alpha_2)^j] \end{aligned}$$

Inserting unity, written as $(1)^{4-j}$, we have the result,

$$\begin{aligned} N'_{\Sigma_1} &= \sum_{j=0}^3 \binom{3}{j} \left[\alpha_2^j \sum_{i=0}^{4-j} \binom{4-j}{i} (1)^{4-j} \alpha_1^i \right. \\ &\quad \left. + L(c_2 \alpha_2)^j \sum_{i=0}^{4-j} \binom{4-j}{i} (1)^{4-j} (c_1 \alpha_1)^i \right] \\ &= (1 - \alpha_1) \sum_{j=0}^3 \binom{3}{j} \alpha_2^j (1 + \alpha_1)^3 \\ &\quad + L(1 + c_1 \alpha_1) \sum_{j=0}^3 \binom{3}{j} (c_2 \alpha_2)^j (1 + c_1 \alpha_1)^3 \\ &= (1 + \alpha_1)(1 + \alpha_1 + \alpha_2)^3 \\ &\quad + L(1 + c_1 \alpha_1)(1 + c_1 \alpha_1 + c_2 \alpha_2)^3. \end{aligned} \quad (9)$$

The fractional saturation of ligand A_1 can now be expressed concisely as

$$\begin{aligned} Y_1 &= \frac{\alpha_1 (1 + \alpha_1 + \alpha_2)^3 + L c_1 \alpha_1 (1 + c_1 \alpha_1 + c_2 \alpha_2)^3}{(1 + \alpha_1)(1 + \alpha_1 + \alpha_2)^3 + L(1 + c_1 \alpha_1)(1 + c_1 \alpha_1 + c_2 \alpha_2)^3}. \end{aligned} \quad (10a)$$

Interchanging subscripts 1 and 2 gives the fractional saturation of ligand A_2 ;

$$\begin{aligned} Y_2 &= \frac{\alpha_2 (1 + \alpha_1 + \alpha_2)^3 + L c_2 \alpha_2 (1 + c_1 \alpha_1 + c_2 \alpha_2)^3}{(1 + \alpha_2)(1 + \alpha_1 + \alpha_2)^3 + L(1 + c_2 \alpha_2)(1 + c_1 \alpha_1 + c_2 \alpha_2)^3}. \end{aligned} \quad (10b)$$

Eqs. (10a) and (10b) have been derived previously by Thompson and ter Bush [19] using ensemble theory.

When discussing the transport capability of hemoglobin for a ligand, in particular oxygen transport, the fraction of all binding sites occupied by the ligand, X_1 , is perhaps more useful than the fractional saturation. This quantity is defined as $X_1 \equiv N_{A_1}/N_\Sigma$. With

$$\begin{aligned} N'_\Sigma &= \frac{N_\Sigma}{4[R_{0,0}]} \\ &= \sum_{j=0}^4 \left[\frac{(4)!}{(4-j)!(j)!} \right] \sum_{i=0}^{4-j} \left[\frac{(4-j)!}{(4-i-j)!(i)!} \right] \\ &\quad \times \left[\alpha_1^i \alpha_2^j + L(c_1 \alpha_1)^i (c_2 \alpha_2)^j \right], \end{aligned}$$

then

$$\begin{aligned} N'_\Sigma &= \sum_{j=0}^4 \binom{4}{j} \sum_{i=0}^{4-j} \binom{4-j}{i} \\ &\quad \times (1)^{4-j-i} \left[\alpha_1^i \alpha_2^j + L(c_1 \alpha_1)^i (c_2 \alpha_2)^j \right] \\ &= \sum_{j=0}^4 \binom{4}{j} \left[\alpha_2^j (1 + \alpha_1)^{4-j} \right. \\ &\quad \left. + L(c_2 \alpha_2)^j (1 + c_1 \alpha_1)^{4-j} \right], \end{aligned}$$

which immediately leads to

$$N'_\Sigma = (1 + \alpha_1 + \alpha_2)^4 + L(1 + c_1 \alpha_1 + c_2 \alpha_2)^4. \quad (12)$$

The quantity X_1 may now be expressed as

$$\begin{aligned} X_1 &= \frac{\alpha_1(1 + \alpha_1 + \alpha_2)^3}{(1 + \alpha_1 + \alpha_2)^4} \\ &\quad + \frac{Lc_1 \alpha_1(1 + c_1 \alpha_1 + c_2 \alpha_2)^3}{(1 + \alpha_1 + \alpha_2)^4} \\ &\quad + \frac{L(1 + c_1 \alpha_1 + c_2 \alpha_2)^4}{(1 + \alpha_1 + \alpha_2)^4}. \end{aligned} \quad (13a)$$

Similarly,

$$\begin{aligned} X_2 &= \frac{\alpha_2(1 + \alpha_1 + \alpha_2)^3}{(1 + \alpha_1 + \alpha_2)^4} \\ &\quad + \frac{Lc_2 \alpha_2(1 + c_1 \alpha_1 + c_2 \alpha_2)^3}{(1 + \alpha_1 + \alpha_2)^4} \\ &\quad + \frac{L(1 + c_1 \alpha_1 + c_2 \alpha_2)^4}{(1 + \alpha_1 + \alpha_2)^4}. \end{aligned} \quad (13b)$$

From the basic definitions of X_1 , Y_1 , etc., one can derive also the symmetrical relations

$$X_1 = \frac{Y_2 - 1}{Y_2 - Y_1^{-1}} \quad \text{and} \quad X_2 = \frac{Y_1 - 1}{Y_1 - Y_2^{-1}} \quad (14)$$

Finally, Thompson and ter Bush [19] have shown that the MWC model is consistent with Haldane's laws when $c_1 = c_2$.

3. Results and discussion

Precise measurement of the oxygenation curve for hemoglobin in blood is complicated by the presence of 2,3-biphosphoglycerate (BPG). In erythrocytes, the molar concentrations of hemoglobin and BPG are comparable, but the molarity of free BPG increases as oxygen binds to the hemoglobin. An additional complication arises by the depletion of BPG on standing and by the presence of small amounts of carboxyhemoglobin and methemoglobin. Nevertheless, a number of careful experimental studies allow one to characterize the Hb-O₂-CO system with a fair degree of confidence. We determined the MWC parameters c_{O_2} , $K_{O_2}^R$ and L from oxygenation data alone and then used these values to select the additional MWC parameters that characterize the presence of carbon monoxide. The oxygenation values used were those of Zijlstra et al. [20] for nine different human blood samples under standard conditions (pH = 7.4, $p_{CO_2} = 40$ torr, $T = 37^\circ\text{C}$) and spanning X_{O_2} values from 0.1 to 0.95. The mean BPG concentration was 4.64 mM. Using these data together with Eq. (13a) for $\alpha_{CO} = 0$, values for L , c_{O_2} and $K_{O_2}^R$ were obtained which minimized S , the sum of the squares of the deviations, between the calculated and experimental X_{O_2} values. The search for the best fit was made systematic by using a three-dimensional grid whose axes were the three parameters above and repeatedly calculating S for 26 neighboring points

about each point, $X_{O_2}\{L, c_{O_2}, \alpha_{O_2}\}$ examined. The grid size was refined as needed to find the best fit (in the least-squares sense). The values found are $L = 4.02 \times 10^7$, $c_{O_2} = 0.00289$ and $K_{O_2}^R = 3.26$ torr. Virtually identical result can be obtained also with the data of Kilmartin [21].

The work of Zijlstra et al. [22] on carboxyhemoglobin provided data for the determination of c_{CO} . Their study gives values of p_{O_2} and X_{CO} at $Y_{O_2} = 0.5$ on 26 blood samples from seven donors at standard conditions. The regression line for their data is

$$P_{50} = 25.5 - 27.0 \cdot X_{CO} \quad (\text{torr}) \quad (15)$$

with a correlation coefficient of 0.98. For a given trial value of c_{CO} , Eqs. (10a) and (13b) were solved together iteratively for α_{O_2} and α_{CO} at $Y_{O_2} = 0.50$ and at X_{CO} values from 0.1 to 0.6 at 0.1 intervals. The least-squares sum, S , was calculated by comparing the iteratively determined values of α_{O_2} and those given by Eq. (15). The Newton–Raphson method [23] was used for all iterative computations. A value of 0.00176 for c_{CO} yielded the best least-squares fit. The average relative difference between p_{O_2} values obtained from Eq. (15) and Eqs. (10a) and (13b) using these parameters is 1.6% over the range of X_{CO} between 0.1 and 0.5.

The effects of carbon monoxide as calculated from Eqs. (13a) and (13b) and corresponding to hemoglobin in blood are shown in Figs. 1–4. Fig. 1 presents the effect of various carbon monoxide pressures on the oxygen saturation curve, X_{O_2} vs. p_{O_2} . These curves are obtained directly from Eq. (13a) for fixed values of α_{CO} . Eq. (13b) is used to obtain the content of Fig. 2 where X_{CO} is plotted as a function of p_{O_2} at different values of α_{CO} . It is generally acknowledged that $K_{CO}^R \approx 225 K_{O_2}^R$ so that the curves in Figs. 1 and 2 correspond to p_{CO} values from approximately 0.0 to 0.50 torr. Fig. 2 reveals a counter intuitive aspect of the Hb–O₂–CO equilibrium. When the CO pressure is below $\alpha_{CO} = 100$, the presence of O₂ first enhances the binding of CO. For example, at $\alpha_{CO} = 50$, the fractional saturation with CO rises by nearly 70% from 0.18 to 0.30 as p_{O_2} increases from 0 to 18 torr. Beyond a certain CO pressure,

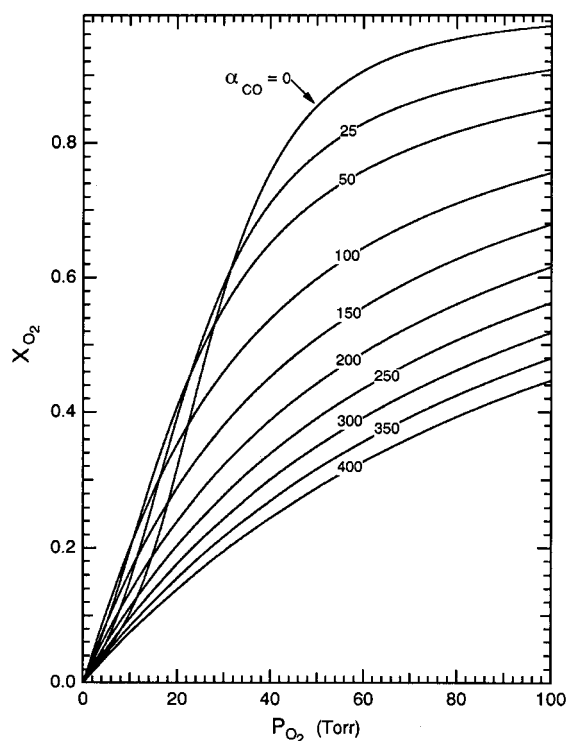


Fig. 1. Oxygenation curves of adult human hemoglobin at different dimensionless pressures, α_{CO} , of CO including $\alpha_{CO} = 0$. The environment is that of the red cell at 37°C, pH of 7.4, 2,3-BPG concentration of 4.64 mM and $p_{CO_2} = 40$ torr.

however, X_{CO} uniformly decreases as p_{O_2} increases. Enhanced CO binding is a reciprocal phenomenon; just as within certain limits oxygen improves carbon monoxide binding, CO, too, increases X_{O_2} below a certain p_{CO} and p_{O_2} . The curves in Fig. 3 are calculated by solving Eq. (13b) iteratively for α_{CO} at fixed values of p_{O_2} and X_{CO} and then determining X_{O_2} directly from Eq. (13a). Enhanced O₂ binding in the presence of small amounts of CO is clearly apparent in the inset of this figure.

The tissue p_{CO} values in a person exposed to a certain environmental p_{CO} can be computed easily using the MWC model. As blood circulates through the lungs, it reaches an equilibrium with the environmental carbon monoxide and the value of X_{CO} approaches that given by Fig. 2. For example, using $K_{CO}^R = 225 K_{O_2}^R$, when the environmental α_{CO} is 75 corresponding to $p_{CO} = 0.101$

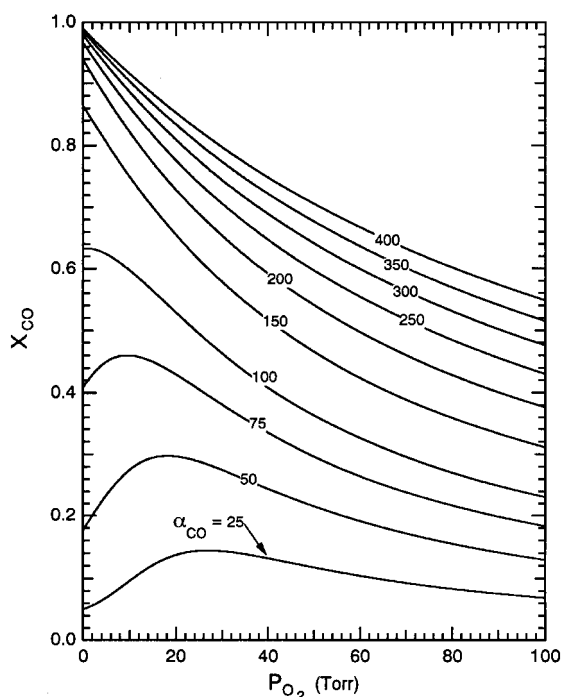


Fig. 2. Variation of the fractional saturation, X_{CO} , with p_{O_2} at different dimensionless carbon monoxide pressures.

torr, and p_{O_2} is 100 torr, X_{CO} becomes 0.182, that is, 18.2% of the total binding sites are occupied by carbon monoxide. The tissue CO pressure then adjusts so as to acquire equilibrium with the $X_{\text{CO}} = 0.182$ value at whatever tissue p_{O_2} is present. If $p_{\text{O}_2}^{\text{tissue}}$ is 40 torr, a typical value in a person at rest, the tissue α_{CO} becomes approximately 37 or 0.05 torr p_{CO} .

Tissue p_{CO} values are plotted as a function of $p_{\text{O}_2}^{\text{tissue}}$ in Fig. 4. An interesting feature is that $p_{\text{CO}}^{\text{tissue}}$ decreases with $p_{\text{O}_2}^{\text{tissue}}$ down to a certain p_{O_2} value; below this, $p_{\text{CO}}^{\text{tissue}}$ increases. The minimum $p_{\text{CO}}^{\text{tissue}}$ moves to slightly lower p_{O_2} values as carboxyhemoglobin concentration rises. Fig. 4 was created by taking the environmental oxygen pressure to be 100 torr and specifying p_{CO} values from which alveolar X_{CO} values can be calculated using Eq. (13b). Since the alveolar X_{CO} is the same as the tissue X_{CO} , the tissue p_{CO} values are determined by iteratively solving Eq. (13b) at specific tissue p_{O_2} values.

Mole fractions of the various species can be

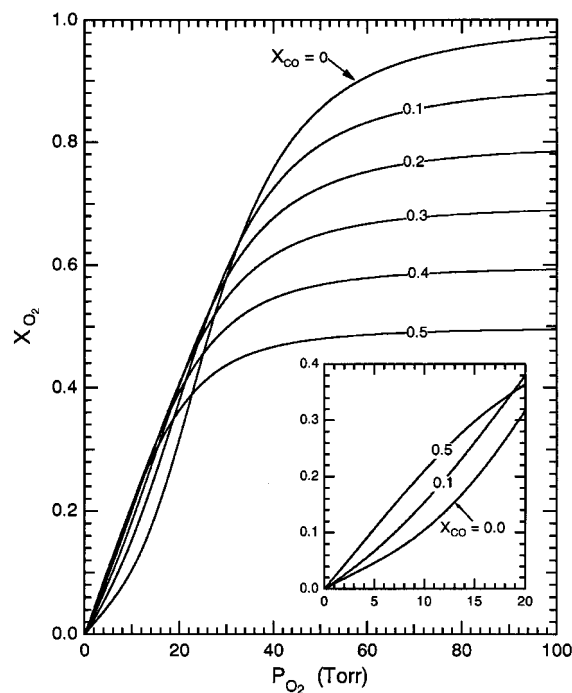


Fig. 3. X_{O_2} vs. p_{O_2} at constant values of X_{CO} . For given tissue or environmental (alveolar) values of X_{CO} and p_{O_2} , the required equilibrium X_{O_2} is determined.

calculated using Eqs. (3a) and (3b) together with Eqs. (13a) and (13b). Figs. 5 and 6 display the mole fractions of various $\text{Hb}(\text{O}_2)_i(\text{CO})_j$ species as a function of p_{O_2} at X_{CO} values of 0.25 and 0.50. Contributions from both T and R states have been combined in these graphs. Singly and/or quadruply liganded species predominate at all ligand compositions. The presence of only small amounts of doubly and triply liganded species is well-known for the MWC model and its extension by Szabo and Karplus [24] for the case of one ligand and is consistent with experimentally determined amounts of intermediate species obtained by Perrella et al. [25] for carbon monoxide binding to hemoglobin. De Cera et al. [18,26] have investigated the binding of oxygen and carbon monoxide, both individually and competitively, to adult human hemoglobin at near standard conditions. Using their Adair constants for the binding partition function obtained for combined experimental data, we calculated mole fractions of the various species for hemoglobin 25%

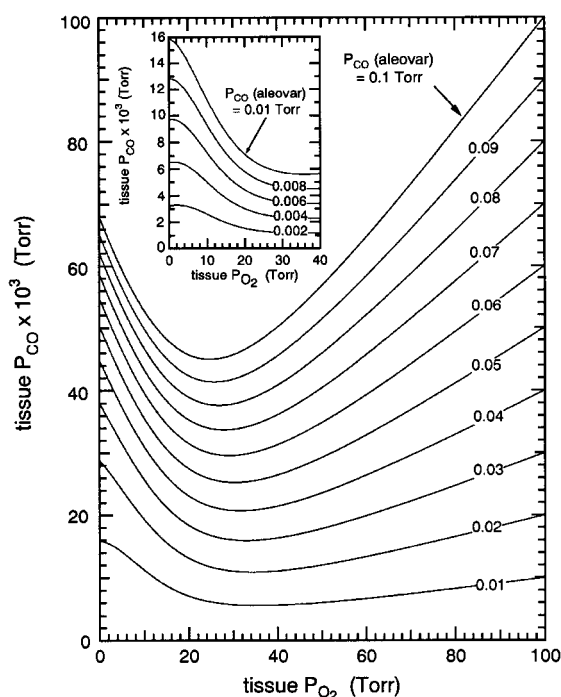


Fig. 4. Dependence of tissue p_{CO} on tissue p_{O_2} at various alveolar p_{CO} values. A value of 100 torr is used for the alveolar p_{O_2} . Here the affinity of R -state hemoglobin for carbon monoxide is assumed to be 225 times that for oxygen.

saturated in oxygen and 25% in carbon monoxide. A comparison of the Adair fits with the MWC model at the same fractional saturation shows that the MWC model retains somewhat more Hb in the unliganded state; the agreement among the remaining species is good except for doubly liganded species. The Adair fits show much more hemoglobin present with two ligands attached than do the MWC equations. This is also the case in the presence of oxygen or carbon monoxide alone. The near absence of double and triply ligated species reflects the strong cooperativity of the MWC model.

The constancy of the Haldane partition coefficient, M , expressed as

$$M = 225 \left(\frac{\alpha_{\text{O}_2}}{\alpha_{\text{CO}}} \right) \left(\frac{X_{\text{CO}}}{X_{\text{O}_2}} \right)$$

was examined for two systems in which the ratios of CO and O_2 bound to hemoglobin are 0.01 and

Table 1

The Haldane M value as a function of total Hb saturation

X_{total}	M	
	$r^a = 0.01$	$r = 0.99$
0.05	141	144
0.10	153	159
0.20	175	179
0.30	188	191
0.40	197	198
0.50	203	204
0.60	208	209
0.70	212	213
0.80	216	216
0.90	220	220
0.95	222	222

^a $r = X_{\text{CO}}/X_{\text{O}_2}$.

$K_{\text{CO}}^R = 225 K_{\text{O}_2}^R$.

0.99. Values for M at different total ligand saturations are given in Table 1. At lower fractional saturation, M differs somewhat for the two systems, converging to the same limiting value as total saturation is reached and Haldane's law is obeyed. Similar results have been reported by Zock [27] in a study based on the Wyman binding potential.

4. Concluding remarks

Following a detailed analysis of data for the binding of CO with hemoglobin, Henry et al. [28] concluded recently that the two-state allosteric model of Monod, Wyman and Changeux 'satisfactorily explains a demanding set of kinetic and equilibrium data, but the fits are not perfect'. A considerable amount of experimental data is now available on the ligation of oxygen and carbon monoxide to hemoglobin. Since one of our aims was to provide saturation curves most useful in human physiology, we chose whole blood data at or near standard physiological conditions. The MWC parameter values $K_{\text{O}_2}^R = 3.26$, $c_{\text{O}_2} = 0.00289$ and the quaternary equilibrium constant, $L = 4.02 \times 10^7$ were determined from oxygenation data alone. The allosteric parameter $c_{\text{CO}} = 0.00176$ was obtained from data fitted to Eq. (15), and based on samples 50% saturated in O_2 . These results are in good agreement with those given by

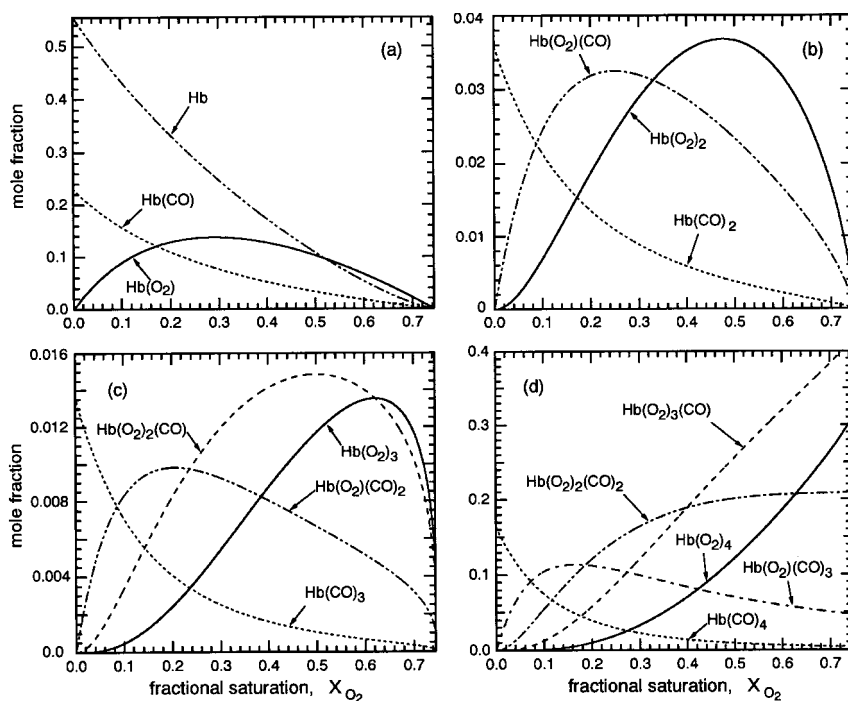


Fig. 5. Mole fractions of the different species as a function of fractional saturation, X_{O_2} at $X_{CO} = 0.25$. These curves are generated from Eqs. (3a),(3b) together with Eqs. (13a),(13b). The plots combine values of $[T_{i,j}]$ and $[R_{i,j}]$: (a) contains Hb and singly liganded species, (b) doubly liganded species, (c) triply, and (d), species with all four ligand sites occupied.

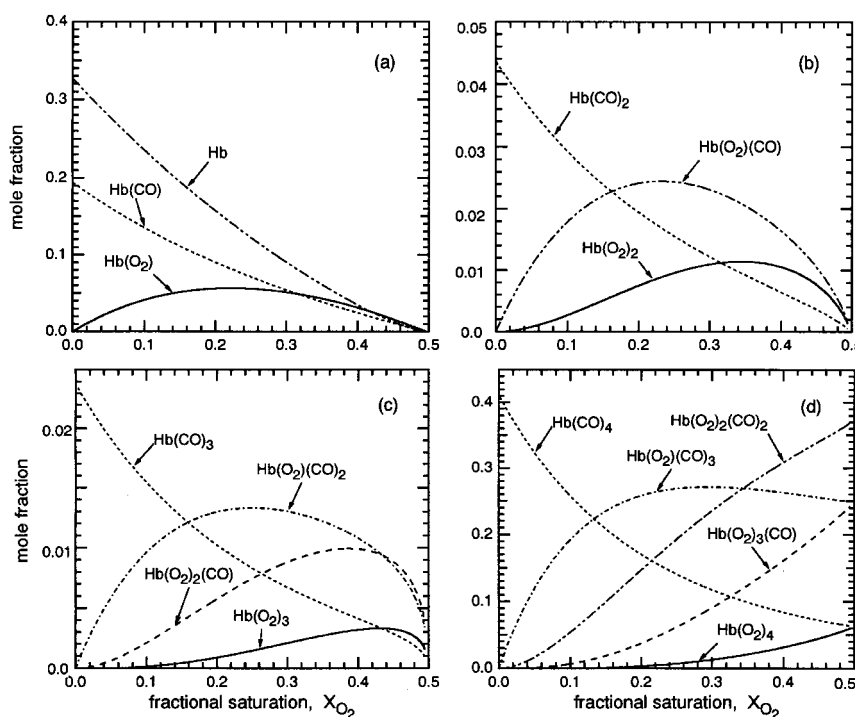


Fig. 6. Mole fractions of various species as a function of X_{O_2} at $X_{CO} = 0.50$ (see Fig. 5 caption).

Henry et al. where the data used was adjusted to slightly different environmental conditions (25°C, 0.1 M Cl⁻) and where oxygen is absent. The values for c_{CO} are almost identical, and those for L , which is very sensitive to environmental conditions, differ by less than a factor of two. The lack of direct CO pressure measurements in our choice of data, however, did preclude the calculation of individual values for K_{CO}^R or K_{CO}^T .

Within the context of CO toxicity, the utility of the MWC model and the equations derived from it lies in establishing quantitative relationships amongst various physiological parameters. Figs. 1–3 display the interdependence between fractional oxygenation, oxygen pressure, and carboxyhemoglobin concentration. A crucial parameter in assessing toxic effects of carbon monoxide is the pressure of this compound in the tissue. Fig. 4 gives this parameter at different environmental levels of CO when the partial pressure of oxygen in the alveoli remains at 100 torr. The equations derived in this study, however, permit construction of similar graphs for any ambient pressure of oxygen. Such graphs can be useful in assessing and interpreting physiological consequences of CO at high altitudes, in hyperbaric chambers, during diving, and in individuals with ailing respiratory function. The rather steep rise in $p_{\text{CO}}^{\text{tissue}}$ below a certain level of tissue oxygenation has not been emphasized before and may be a key factor in understanding chronic low level CO poisoning.

References

- [1] C.G. Douglas, J.S. Haldane, J.B.S. Haldane, *J. Physiol. (London)* 44 (1912) 275.
- [2] F.J.W. Roughton, R.C. Darling, *Am. J. Physiol.* 141 (1944) 17.
- [3] M.P. Hlastala, in: H.D. Patton, A.F. Fuchs, B. Hille, A.M. Sher, R. Steiner (Eds.), *Textbook of Physiology*, vol. 2, Circulation, Respiration, Body Fluids, Metabolism and Endocrinology, W.B., Saunders Co., Philadelphia 1989, p. 1017.
- [4] R.F. Coburn, H.J. Forman, in: A.P. Fishman, L.E. Farhi, S.M. Tenney, S.R. Geiger (Eds.), *Handbook of Physiology*, section 3, The Respiratory System, vol. IV, Gas Exchange, Am. Physiol. Soc., Bethesda, MA, 1987, p. 439.
- [5] J.F. Nunn, *Nunn's Applied Respiratory Physiology*, 4th ed. Butterworth-Heinemann Ltd., 1993, p. 280.
- [6] J. Monod, J. Wyman, J.P. Changeux, *J. Mol. Biol.* 12 (1965) 88.
- [7] S.J. Edelstein, *Nature* 230 (1971) 224.
- [8] J.J. Hopfield, R.G. Shulman, S. Ogawa, *J. Mol. Biol.* 61 (1971) 425.
- [9] A. Levitzki, *Quantitative Aspects of Allosteric Mechanisms*, Springer-Verlag, Berlin, 1978, p. 32.
- [10] J. Brouwer, C. Bonaventura, J. Bonaventura, in: C. Bonaventura, J. Bonaventura, S. Tesh (Eds.), *Physiology and Biology of Horseshoe Crabs*, Alan R. Liss, New York, 1982, p. 231.
- [11] K. Imai, *Allosteric Effects in Hemoglobin*, Cambridge University Press, 1982, p. 108, 114.
- [12] B. Richey, H. Decker, S.J. Gill, *Biochemistry* 24 (1985) 109.
- [13] S.J. Edelstein, J.T. Edsall, *Proc. Nat. Acad. Sci. USA* 83 (1986) 3796.
- [14] G. Zhou, P.S. Ho, K.E. van Holde, *Biophys. J.* 55 (1989) 275.
- [15] F.J.W. Roughton, *Ann. N.Y. Acad. Sci.* 174 (1970) 177.
- [16] Y. Okada, I. Tyuma, Y. Ueda, T. Sugimoto, *Am. J. Physiol.* 230 (1976) 471.
- [17] M.P. Hlastala, H.P. McKenna, R.L. Franada, J.C. Deter, *J. Appl. Physiol.* 41 (1976) 893.
- [18] E. Di Cera, M.L. Doyle, P.R. Connally, S.J. Gill, *Biochemistry* 26 (1987) 6494.
- [19] C.J. Thompson, R. ter Bush, *J. Theor. Biol.* 34 (1972) 441.
- [20] W.B. Zijlstra, G. Kwant, S. Oeseburg, A. Zwart, in: A. G. Schneck, C. Paul (Eds.), *Hemoglobin*, Editions de l'Université de Bruxelles, Brussels, 1984, p. 63.
- [21] J.V. Kilmartin, *Br. Med. Bull.* 32 (1976) 209.
- [22] W.G. Zijlstra, A. Buursma, G. Kwant, B. Oeseburg, A. Zwart, *Advan. Exp. Med. Biol.* 191 (1985) 533.
- [23] W.H. Press, S.A. Teukolsky, W.T. Vetterling, B.P. Flannery, *Numerical Recipes in FORTRAN*, 1992, p. 355.
- [24] A. Szabo, M. Karplus, *J. Mol. Biol.* 72 (1972) 163.
- [25] M. Perrella, L. Sabbioneda, M. Samaja, L. Rossi-Bernardi, *J. Biol. Chem.* 261 (1986) 8391.
- [26] E. Di Cera, M.L. Doyle, M.S. Morgan, et al., *Biochemistry* 28 (1989) 2631.
- [27] J.P. Zock, *Advan. Exp. Med. Biol.* 277 (1990) 199.
- [28] E.R. Henry, C.M. Jones, J. Hofrichter, W.A. Eaton, *Biochemistry* 36 (1997) 6511.